JOURNAL OF PROPULSION AND POWER
Vol. 23, No. 2, March–April 2007

Decomposition of Aluminum Hydride Under Solid Rocket Motor Conditions

Tim Bazyn,* Herman Krier,† Nick Glumac,‡ Nagraj Shankar,§ X. Wang,‖ and Thomas L. Jackson¶
University of Illinois at Urbana–Champaign, Urbana, Illinois 61801

DOI: 10.2514/1.22920

The decomposition rate of aluminum hydride powder was measured at slightly elevated temperatures (400–500 K) using the pressure rise due to the released hydrogen. This information is important for understanding the combustion behavior of aluminum hydride when used in propellants and explosives. The thermolysis measurements fit well to an Arrhenius-type exponential fit, with a preexponential of 3.29e9 1/s and an activation energy of 97.6 kJ/mol. Two-dimensional simulations of aluminum particles in a propellant mixture were also performed to determine the temperature and velocity history of the particles in a burning propellant. Using this information and extrapolating the measured dehydrogenation rates, it was determined that alane will decompose before being ejected off of the propellant surface. This prediction suggests that the hydrogen will be available to react in the primary flame zone of the rocket motor, and will thus impact the stoichiometry in this region. The decomposition process could also affect the surface characteristics of the burning propellant.

I. Introduction

ALUMINUM hydride has been proposed as a propellant additive for solid rocket motors (SRMs) due to its high energy content. Aluminum hydride, also known as alane, has a chemical formula of AlH_3 and exists in seven different crystalline phases, but the α-phase is the most stable phase. Details on the synthesis and structure of the other alane phases are provided in [1]. The α-phase can be made more stable using technology developed in the former Soviet Union and described in US Patent 6228338 B1 [2]. The thermodynamic properties of aluminum hydride were experimentally determined by Sinke et al. [3]. The heat of formation was found to be approximately −2.7 kcal/mol. Calculations using the ProPEP code [4] reveal that a roughly optimized mixture of aluminum hydride with hydroxyl-terminated poly-butadiene (HTPB) and ammonium perchlorate (AP) yields an 8% increase in specific impulse over an optimized mixture of aluminum, HTPB, and AP. These calculations show that alanized propellants produce combustion products with lower molecular weight and slightly increased temperature as compared to the aluminized propellant. Clearly, alane usage in propellants has the potential to lead to significant improvement in SRM performance.

Whereas the thermodynamic calculations indicate large gains in specific impulse, poor combustion properties, such as a slow burning rate or large pressure exponent, would significantly impact the actual gains observed in alane propellant performance. In a previous work [5], the combustion characteristics of aluminum hydride were examined. Under conditions similar to SRM's, alane was determined to react in a two-step fashion:

$$AlH_3(s) \rightarrow Al(s) + 3/2H_2(g) \qquad \text{(decomposition)} \qquad (1)$$

$$Al + 3/4O_2 \rightarrow 1/2Al_2O_3 \qquad \text{(oxidation)} \qquad (2)$$

Step 1 occurs very fast at the elevated temperatures and pressures found in SRM conditions. The hydrogen desorbs from the particle and has time to diffuse away from the particle surface. The oxidation of aluminum then occurs on longer timescales. Bazyn et al. [5] illustrated that the combustion timescales and temperatures were nearly indistinguishable between alane and aluminum. Because the dehydrogenation occurs much faster than the aluminum oxidation, the aluminum oxidation of alane combustion appears to be practically identical to similarly sized aluminum particle combustion.

Whereas this result illustrates that the oxidation of the aluminum found in alane will behave similarly to aluminum when used in a SRM propellant, the behavior of the desorbed hydrogen in a SRM propellant remains uncertain. Particularly, the availability of the hydrogen to react in the primary flame zone, where the oxidizer and binder react, is uncertain. This availability depends on the decomposition timescales. If decomposition occurs early enough, the hydrogen will desorb while the particle is still on the propellant surface or immediately after the particle is ejected from the particle surface. In this case, the primary flame stoichiometry will be affected by the hydrogen gas. Conversely, if the decomposition timescales are slow enough that the alane particles pass through the primary flame zone intact, the hydrogen will then desorb in the post flame region. In this region, the hydrogen gas will be exposed to a region consisting primarily of N_2, HCl, CO_2, and H_2O, and these gases will not react considerably with the hydrogen gas. The H_2 would then pass through the rocket motor and exit out of the nozzle. These two limiting scenarios demonstrate that knowing the decomposition timescale is imperative to designing propellants using alane.

Previously, the thermolysis rate measurements were attempted in a heterogeneous shock tube [5]. The 10 μm particles were dehydrogenated behind the incident shock at 1500 K and 1 atm. The desorbed hydrogen gas reacted with ambient oxygen, and the resulting emission of OH was observed at 310 nm. The time resolution of these measurements was limited by the rate at which the hydrogen reacts to form OH and the time for the shock to pass the particle cloud. Therefore, these measurements provided an upper bound of 100 μs on the dehydrogenation time under these conditions. The decomposition time was found to be quite fast, but more accurate predictions could not be made.

Received 2 February 2006; accepted for publication 23 June 2006.

*Ph.D., Mechanical and Industrial Engineering, 1206 West Green Street. Member AIAA.
†Professor, Mechanical and Industrial Engineering, 1206 West Green Street. Fellow AIAA.
‡Associate Professor, Mechanical and Industrial Engineering, 1206 West Green Street. Member AIAA.
§Ph.D. Candidate, Mechanical and Industrial Engineering, 1206 West Green Street.
‖Scientist, Center for Simulation of Advanced Rockets, 1304 West Springfield Avenue. Member AIAA.
¶Senior Research Scientist, Center for Simulation of Advanced Rockets, 1304 West Springfield Avenue. Associate Fellow AIAA.

Previous studies have examined the timescales of hydrogen release from aluminum hydride. Ismail and Hawkins [6] examined the nonisothermal decomposition reaction using vacuum thermal stability (VTS) and thermogravimetric analysis (TGA). During dehydrogenation, the porosity initially increases, followed by a decrease in particle size and eventual closing of the pores. The kinetic data were analyzed using the ASTM method assuming model free kinetics for comparison purposes, which yielded an activation energy of 97.0 ± 3.1 kJ/mol. Analysis using the Friedman method suggested a two-step mechanism, so a two-step model was proposed consisting of nucleation and growth. The nucleation step was found to be the rate limiting step with an activation energy of either 83.8 or 99.0 kJ/mol, depending on the model assumed for the second step (which has a significantly lower activation energy).

Tarasov et al. [7] examined the isothermal decomposition of alane using nuclear magnetic resonance. This study examined the effects of temperature and particle size, and compared the decomposition of aluminum hydride to aluminum deuteride. They fit their decomposition curves to three steps: induction, acceleration, and deceleration, with activation energies for each process of 97, 112, and 108 kJ/mol, respectively. Particle size is shown to affect the decomposition time significantly, with increasing particle size causing longer decomposition times. Their data indicate that the relationship can be approximated as decomposition time being proportional to particle diameter to the 0.8–1.0 power.

Mikhailov et al. [8–10] used optical absorption, electrical conductivity, and gas evolution measurements of aluminum hydride during photolysis and thermolysis to understand the underlying processes. The absorption differences between the UV-irradiated and unirradiated samples indicated that different physical processes are occurring during thermolysis and photolysis. The authors suggest that the decomposition involves both nucleation and growth, and that nucleation is the rate limiting step in thermal decomposition and growth is the limiting step in irradiated samples. In another study by the same group, Poshevnev et al. [11] use gas evolution to determine the very early thermolysis behavior of aluminum hydride at temperatures below 100°C.

Herley et al. [12,13] examined the decomposition of alane isothermally at 140°C both with and without the presence of γ-radiation. The decomposition curves were fit to three stages, with a power law describing an induction period and with separate Avrami–Erofeyev rate equations describing both the acceleration and decay periods. The data indicate that the irradiated sample decomposes roughly four times faster than the unirradiated sample. The activation energies for the rate constants in their fits for new and aged powder, respectively, were determined to be 107.0 ± 11.0 and 96.1 ± 4.4 kJ/mol for the induction period, 150.3 ± 10.0 and 158.0 ± 12.0 kJ/mol for the acceleratory period, and 162.0 ± 11.3 and 164.0 ± 9.0 kJ/mol for the decay period.

Zakharov and Tshkhai [14] looked at the decomposition of solvated aluminum hydride. Two distinct events were observed, which were suspected to be desolvation followed by decomposition, which had an activation energy of 72.2 ± 2.5 kJ/mol.

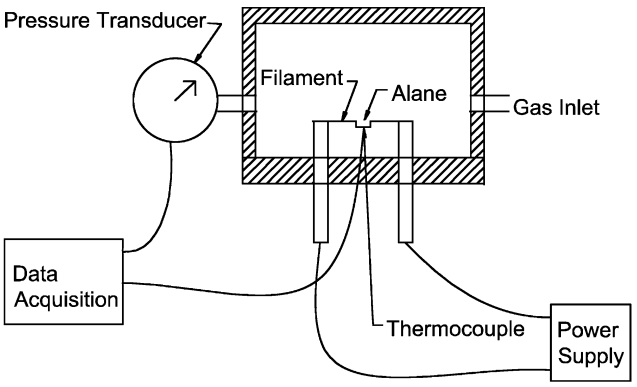

Fig. 1 Schematic of the setup used for the thermolysis kinetics measurements.

VTS was also measured at 60°C in the US Patent 6228338 B1 [2] of stabilized and unstabilized aluminum hydride. The stabilized alane took approximately 13 days to obtain 1% decomposition, which was roughly 25% better than the unstabilized material.

This work deals with the accurate determination of decomposition time at temperatures slightly higher than those previously recorded. This information will provide information on the decomposition of aluminum hydride at temperatures closer to those relevant to the performance of the material in a SRM. The measured rate of decomposition in conjunction with the temperature history of a particle inside a solid rocket motor as calculated by a detailed computational model is used to estimate the behavior of alane in rocket applications. From this analysis, the relative influence of hydrogen on the primary flame stoichiometry is examined.

II. Experimental Approach

The decomposition time was determined for a small amount of aluminum hydride powder heated on a molybdenum or stainless steel filament. As the hydrogen gas desorbs from the particles, the pressure in the small chamber increases, and this pressure increase is measured as an indicator of decomposition. The experimental configuration is shown schematically in Fig. 1. The stainless steel chamber has a volume of approximately 15 cm^3, which is small enough for a 1 mg sample of alane to generate an appreciable pressure rise in the chamber when dehydrogenated.

Typically, a few milligrams of powder were spread in an indentation on the metal filament near (± 2.5 mm) the center of the filament. The powder loading is such that there is approximately a single layer of alane covering the indentation so that particles will be heated at approximately the same rate as the filament, and the time lag between the filament and the particle temperatures is much less than the test times. The chamber was first evacuated and filled with argon to create an inert environment. The filament power supply was then turned on, and the filament reached the stable temperature set point in approximately 1 s. The temperature of the filament was measured via a thermocouple with a 0.70 mm bead diameter. The heat up time of the filament limited the minimum measurable decomposition time.

The decomposition time of the material is measured via the pressure vs time history in the chamber. Because the temperature of the gas surrounding the filament increases as the filament is heated, there is an increase in the pressure of the chamber due solely to the temperature increase. This temperature increase was measured and determined to be only a function of the filament temperature. Therefore, the filament temperature is measured during the event, and the pressure increase due to the temperature of the filament is determined. This pressure rise is subtracted from the raw pressure signal, yielding the pressure rise due to the desorbed hydrogen. This signal is then analyzed for the decomposition time. The decomposition times reported here are the time for 90% of the pressure rise, and thus 90% of the decomposition, to occur. The mass of the sample and the pressure rise were also checked to verify the completeness of the reaction.

The temperature profile of the filament was measured in the region near the center of the filament. The region within 2.5 mm of the center of the filament was found to be well within 3% of the peak temperature. Therefore, all of the particles placed in the indentation are exposed to temperatures within 3% of the peak temperature. Whereas the voltage of the resistive heating power supply remained approximately constant, the temperature of the filament had some random fluctuations. Therefore, the total error of the temperature is a combination of the 3% spatial error across the filament and the measured fluctuation in the temperature during the decomposition time. The error in decomposition time is fairly small, with the heat up time the primary source of uncertainty. This error is estimated at ± 2 s.

The AlH_3 sample used in the current investigation was characterized using scanning electron microscopy (SEM) and x-ray diffraction (XRD). The SEM (Hitachi 4700 FESEM operating at 20 keV) analysis clearly indicates that the AlH_3 powder sample primarily consists of rhombohedral crystals with a mean size of

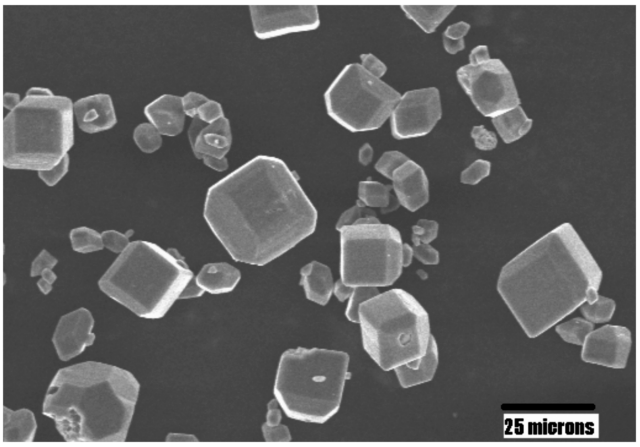

Fig. 2 SEM of the α-AlH_3 used in this study.

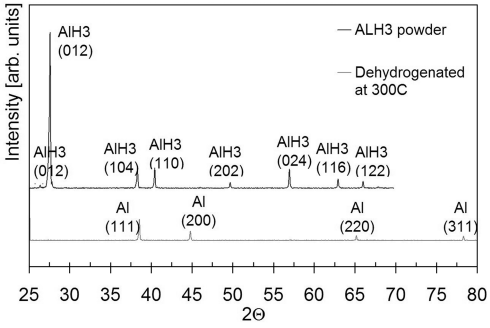

Fig. 3 XRD analysis of aluminum hydride before and after thermal decomposition.

approximately 20 μm (see Fig. 2). An elemental analysis by energy dispersive x-ray spectroscopy (EDX) within the SEM reveals that the measurable elements near the powder surface are Al, O, and N in a 82/10/8 ratio, with no detectable trace of carbon or other potential solvent residuals from the alane formation. H, however, could not be detected using this technique. Further elemental analysis of the sample was performed using a glancing angle XRD (Rigaku DMAX) with a Cu–K_α source at 45 kV and 20 mA using 1 deg inlet and 0.3 deg outlet slits and with a scanning rate of 1 deg / min. As seen in Fig. 3, the XRD data suggest that the dominant phase is rhombohedral AlH_3 (according to the Joint Committee on Powder Diffraction Standards card nos. 71-2422). Based on the SEM and XRD data, the AlH_3 powder samples used in this work are primarily crystalline rhombohedral AlH_3 with contamination levels of less than 1 wt%. The AlH_3 powders are possibly covered with a thin oxide or other coating as indicated by the EDX. The presence of surface adsorbed hydrocarbons could not be detected using the present characterizing schemes; however, if present, the amount (less than 1 wt.% of AlH_3) is very small compared to the bulk phase. The weight of the powder was also measured before thermolysis experiments, and the desorbed gas pressures indicate that the original material is nearly completely (>90% in all cases) alane. There is no visible initial rise corresponding to out gassing of solvents as observed in [14].

III. Experimental Results

The 90% decomposition time was measured for temperatures in the 400–500 K range. This upper temperature is limited by the fast decomposition time, which approaches the heat up time of the filament. The measured decomposition times are shown in Fig. 4. The data are displayed as $1/t_{\mathrm{dh}}$, the 90% decomposition time in seconds, vs 10^3/Temperature in K. The line on the plot represents an Arrhenius-type fit to the data of the following form:

$$r_{\mathrm{dh}} \propto 1/t_{\mathrm{dh}} = Ae^{-E_a/RT} \tag{3}$$

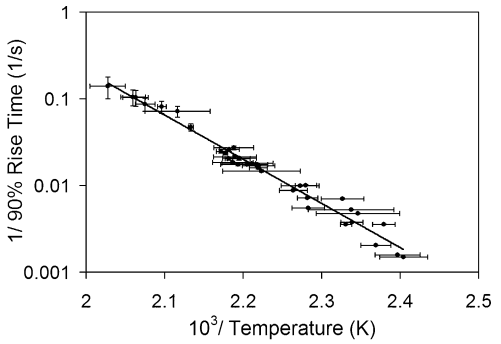

Fig. 4 Arrhenius-style plot of 1/90% rise time vs 10^3/Temperature.

where r_{dh} is the decomposition rate, A is a preexponential constant, E_a is an activation energy, and R is the universal gas constant. For these data, the best fit corresponds to $A = 3.29\mathrm{e}9$ 1/s and $E_a = 97.6$ kJ/mol. The 90% confidence intervals for these two fit parameters are $9.85\mathrm{e}8$ 1/s $< A < 1.10\mathrm{e}10$ 1/s and 93.1 kJ/mol$< E_a <$ 102 kJ/mol. This fit can be seen to give an excellent prediction of the decomposition behavior. These measurements agree well with other reported measurements. Whereas this analysis assumes a simple, single-step rate equation, the more complicated fits in [6] all indicate that nucleation is the rate limiting step at lower temperatures and will continue dominate at higher temperatures. The single-step analysis of Ismail and Hawkins [6] yields an activation energy of 97.0 ± 3.1 kJ/mol, which agrees very well with our measurements. Our measurements also agree reasonably well with the rate limiting step of their more complicated, two-step models of [6]. Extrapolation of Eq. (3) yields faster decomposition than other lower temperature measurements [7,10,12,13], although that is possibly because of the growth rate becoming more important at lower temperatures and because of the smaller particle size used in this study as compared to the references. When extrapolated to room temperature, the decomposition time is on the order of years, which seems to agree with observations of long-term stability. When extrapolated to 333 K, the measurements agree reasonably well with information provided in US Patent 6,228,338 B1 on the process to produce alane [2].

IV. Analysis

The measured decomposition times can now be used to predict the appearance and availability of the desorbed hydrogen in an SRM application. The first step in this process is to determine the temperature history of a particle embedded in a SRM propellant as the surface burns and the particle is released into the combustion chamber. A model of the aluminum or alane particle behavior in a typical solid rocket propellant developed by Center for Simulation of Advanced Rockets (CSAR) was used to determine the location and temperature of the particle as it is ejected from the particle surface and flows through the combustion chamber. The next step is to then extend the relation given in Eq. (3) to the temperatures seen by the particles. This rate equation can be integrated with the temperature history of the particle, and the time and location of the dehydrogenation process can be determined. The details of this analysis will be given in the following subsections.

A. Model Development

In recent years a considerable amount of effort has been dedicated to computational simulations of heterogeneous solid propellant combustion. A variety of tools have emerged from these studies. The most important are the modeling of propellant morphology [15,16], homogenization [17], and an unsteady two- and three-dimensional combustion model with complete coupling between the solid and gas phases [18–20]. Our code accounts for the unsteady multidimensional heat conduction in the solid with different conductivities for different materials, combustion in the gas phase with temperature-dependent transport parameters and Arrhenius kinetics, pyrolysis

laws at the surface of Arrhenius form that relate the local regression speed to the surface temperature, and proper connection conditions across the solid–gas interface. In the solid, a model of the propellant morphology uses random packs of spheres (3-D) or cylinders (2-D). These tools have been applied to the study of nonaluminized heterogeneous propellants, including the periodic sandwich (a periodic array of alternating AP and binder slices) and disks or spheres randomly packed. Comparisons of surface profiles to those of experimental observations for sandwich configurations and comparisons to experimental burn rates for a variety of propellant compositions over a wide pressure range are very encouraging and suggest that multidimensional numerical simulation is a viable tool for understanding combustion characteristics of composite propellants.

The first studies employed a body-fitted grid along the moving interface by means of a mapping technique when the surface is single valued. The computational difficulties are significantly increased when the burning surface undergoes a complex or multivalued shape. Such shapes can arise, for example, when aluminum particles are embedded in the propellant. In this case the mapping strategy must be abandoned in favor of a more general interface capturing method. One such method, level sets, is presented in [21,22]. In these works a low Mach number Navier–Stokes solver is implemented and coupled with the level set method. By comparing results obtained by the level set method with those of the previous body-fitted code, it has been demonstrated that the algorithm works quite well when the gas and solid phases are completely coupled.

The purpose here is to extend the two-dimensional version of the code to investigate the temperature history of aluminum hydride particles embedded in an AP/HTPB composite propellant. Results of the simulations are presented next.

B. Model Results

Any serious attempt to describe the characteristics of heterogeneous propellants must include a packing algorithm, a strategy for defining and constructing a model propellant. Lattice (or crystal) packs are easily defined, but do not reflect the random nature of a true propellant. For this, a random packing algorithm must be used, and a suitable one is defined and discussed in [15,16]. This algorithm is dynamic in nature and can closely pack spheres or discs of arbitrary size within a periodic domain. Packs generated in this fashion can be designed to capture the volume fractions of various sized particles in experimental or industrial packs.

We used the packing algorithm to generate two-dimensional packs of the kind shown in Fig. 5. The first case examined is a single aluminum hydride particle embedded in a bimodal AP pack. The AP particles in the solid are outlined in white, and the aluminum hydride particle is outlined in black. Each pack consists of 36 particles: 4 AP particles of diameter 200 microns and 32 AP particles of diameter 50 microns. The relative AP volume fractions are 10% 200 μm and 90% 50 μm, for a total volume fraction of 76% of the solid. To account for the single aluminum hydride particle, a single 50 μm AP particle was removed from near the center of the pack and replaced by a single aluminum hydride particle of various diameters. The net effect of this is to reduce the AP volume fraction slightly. The dimensions of the pack are kept fixed at 498×498 μm. The aluminum hydride particle was modeled as a disk, with diameters of 8, 16, 32, and 64 microns. The thermal conductivity of aluminum hydride, which is not well known, is assumed to be that of aluminum as a first-order approximation.

The combustion code is started with the surface located initially at the top of the pack, and the pack is allowed to burn downward through the solid until a few milliseconds after detachment. At this time the particle has become detached from the surface and is moving upwards through the gas phase as dictated by the local forces acting on the particle. The background pressure is held fixed at 20 atm. Temperature contours for each particle at an instant of time are shown in Fig. 6. At this instant of time the aluminum hydride particle is located on the surface, before detachment. The propellant surface is shown by the thick, black curve. Note that the surface is not flat but highly corrugated. This is due to the heterogeneity of the pack, which supports both premixed and diffusion flames in the gas phase. The temperature history of the particle is followed and plotted in Fig. 7, and the corresponding velocity history is shown in Fig. 8. The temperature histories are used in the next section to predict decomposition.

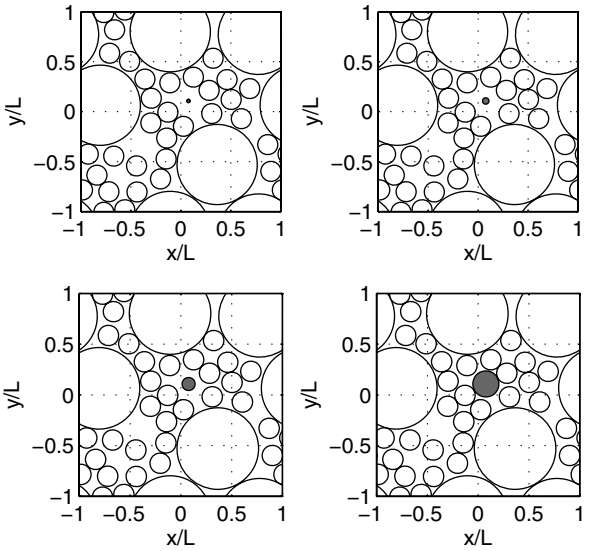

Fig. 5 Structure of 2-D packs of AP particles and HTPB binder (voids) with a single embedded aluminum hydride particle (filled) with diameter of 8 μm (upper left), 16 μm (upper right), 32 μm (bottom left), and 64 μm (bottom right).

The preceding case was selected because it highlighted the effects of a single particle. However, in a real propellant, particles are usually clumped together and form "pockets," as dictated by the coarse AP particles. Therefore, we also considered the case of a number of particles embedded in an AP/HTPB propellant. Agglomeration is ignored in the present study because the physics are not yet well understood, and also because the present code cannot handle particle merging. Figure 9 shows the propellant morphology. The pack consists of 175 particles: 4 AP particles of diameter 200 microns, 19 AP particles of diameter 50 microns, and 152 aluminum hydride particles of diameter 16 microns. The total AP volume fraction is 64% and the volume fraction of the particles is 12%, for a total volume fraction of 76% of the solid. The dimensions of the pack are 504.6×504.6 μm. As before, the combustion code is started with the surface located initially at the top of the pack, and the pack is allowed to burn downward through the solid. During this time a number of particles have become detached from the surface and move upwards through the gas phase as dictated by the local forces acting on each particle. The background pressure is held fixed at 20 atm. Temperature contours at an instant of time are shown in Fig. 10. The propellant surface is shown by the thick, black curve. Note that the surface is not flat but highly corrugated and is due to the heterogeneity of the pack, which supports both premixed and diffusion flames in the gas phase. The velocity, location, and temperature history of a group of particles are followed and plotted in Fig. 11. The temperature histories are used in the next section to predict decomposition.

C. Decomposition Prediction

Using the results predicted by the computational model, we can then apply Eq. (3) to the predicted temperature vs time histories. To do this, the exponential behavior observed at lower temperature must be extrapolated to higher temperatures (e.g., $\sim$800 K). Though this is a common practice in energetic materials rate predictions, it remains an assumption. The possible consequences of this assumption are qualitatively discussed later.

The results from the model give the time-location-temperature history of many aluminum hydride particles within the packed

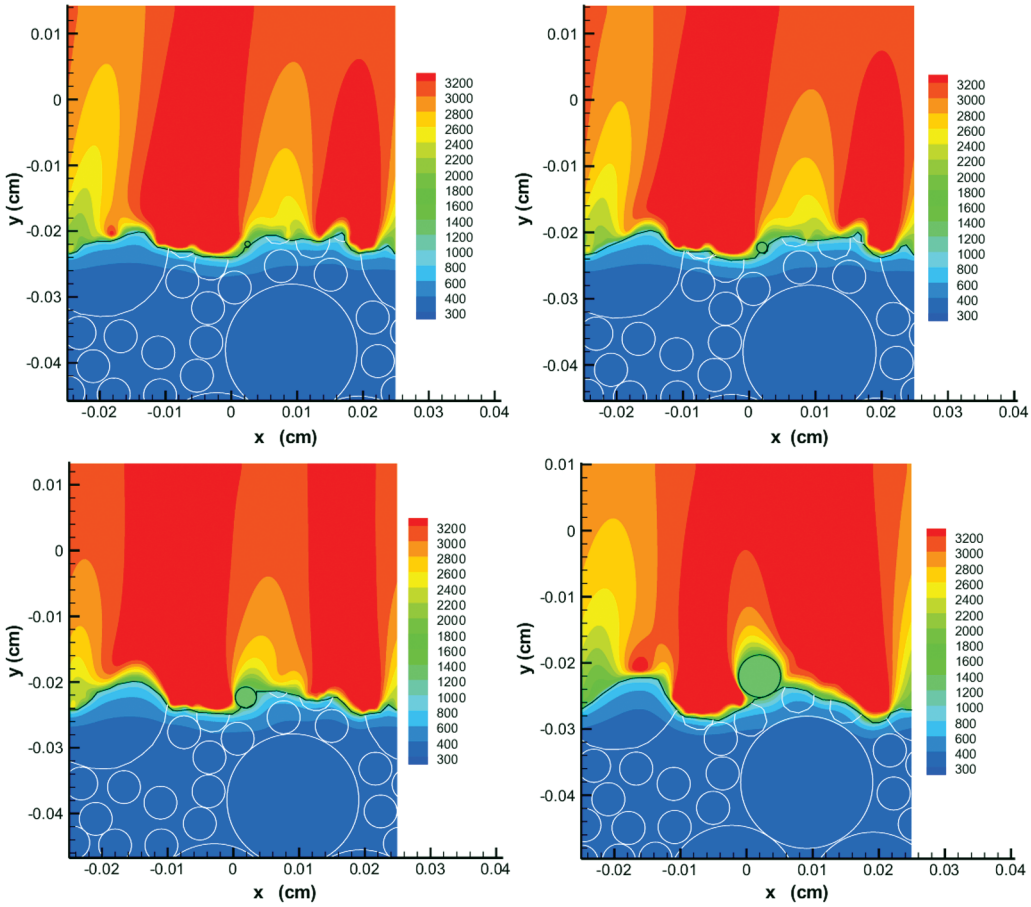

Fig. 6 Instantaneous temperature contours for the two-dimensional packs of Fig. 5 at a pressure of 20 atm; 8 μm diameter (upper left), 16 μm diameter (upper right), 32 μm diameter (bottom left), and 64 μm diameter (bottom right).

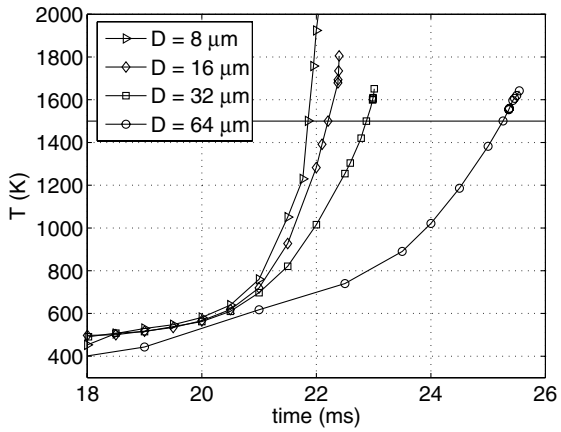

Fig. 7 Temperature history of a single alane particle embedded in a heterogeneous AP/HTPB pack.

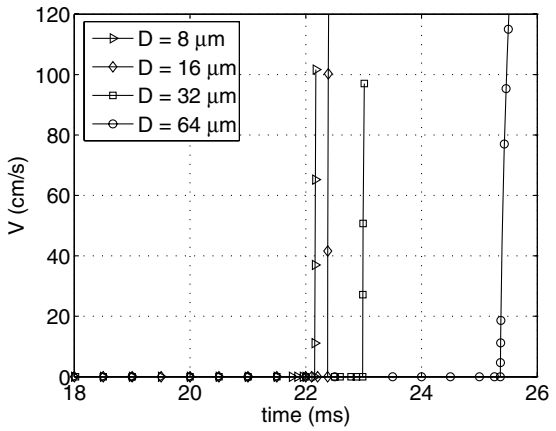

Fig. 8 Velocity history of a single alane particle embedded in a heterogeneous AP/HTPB pack.

propellant. Two sample particle temperature histories, along with the predicted dehydrogenation behavior using Eq. (3) based on these temperature profiles, are shown in Fig. 12. These profiles result from a simulation of a heterogeneous pack of aluminum hydride, AP, and HTPB. Ten of the aluminum hydride particles in the pack were followed to extract the temperature and velocity histories. Figure 12a represents that particle that had the most rapid temperature rise while in the propellant surface, whereas Fig. 12b shows the particle that had the most gradual temperature rise. The temperature profiles terminate when the particle is ejected from the propellant surface. Therefore, the plots represent behavior of the particle while still in the attached to the propellant surface. As can be seen, the decomposition occurs while the particle is still attached to the propellant surface. For the entire sample of ten particles in the 2-D pack of Al/AP/HTPB, the simulations show that decomposition will occur well before the particle is ejected from the propellant surface.

Figure 7 showed that different sized particles will have significantly different temperature histories. Small particles will be contained completely within the melt layer, and will more closely follow the temperature of the surrounding propellant. Larger particles will exist adjacent to the solid, liquid, and gas phases of the propellant simultaneously. Thus, the temperature rise in the large particle cases is significantly more gradual. Figure 13a shows the temperature history and predicted decomposition behavior of an 8 μm alane particle. Because of the exponential dependence on

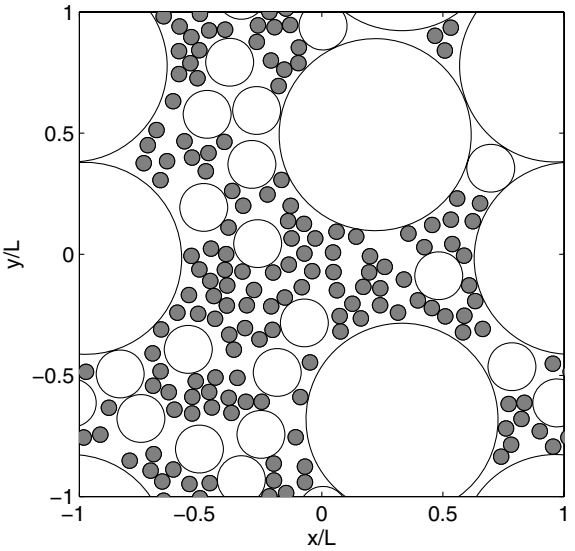

Fig. 9 Structure of the 2-D pack of AP particles and HTPB binder (void) with alane particles (filled).

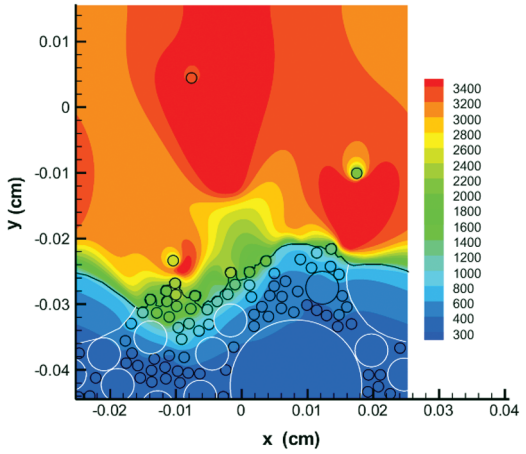

Fig. 10 Instantaneous temperature contours for the 2-D pack of Fig. 9 at 20 atm; alane particles are outlined in black, AP in white.

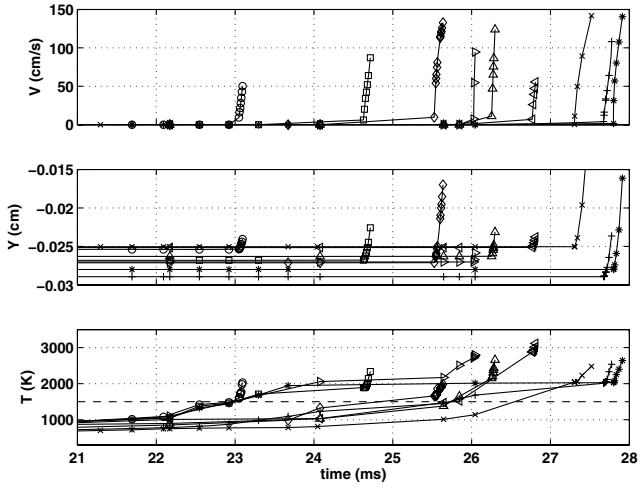

Fig. 11 Velocity (top), height above propellant surface (middle), and temperature (bottom) history for nine alane particles of Fig. 10.

temperature, decomposition is negligible until the particle is close to the propellant surface. The figure shows that the once the temperature rises significantly, the dehydrogenation occurs very rapidly. The simulations show that the dehydrogenation definitely occurs while

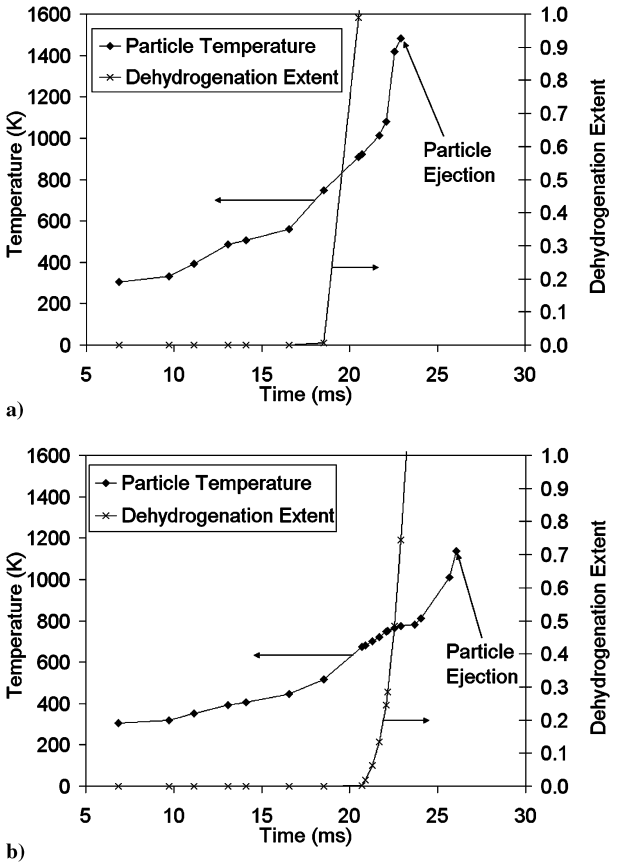

Fig. 12 Plot of particle temperature and dehydrogenation extent vs time for two particles in the packed propellant simulations.

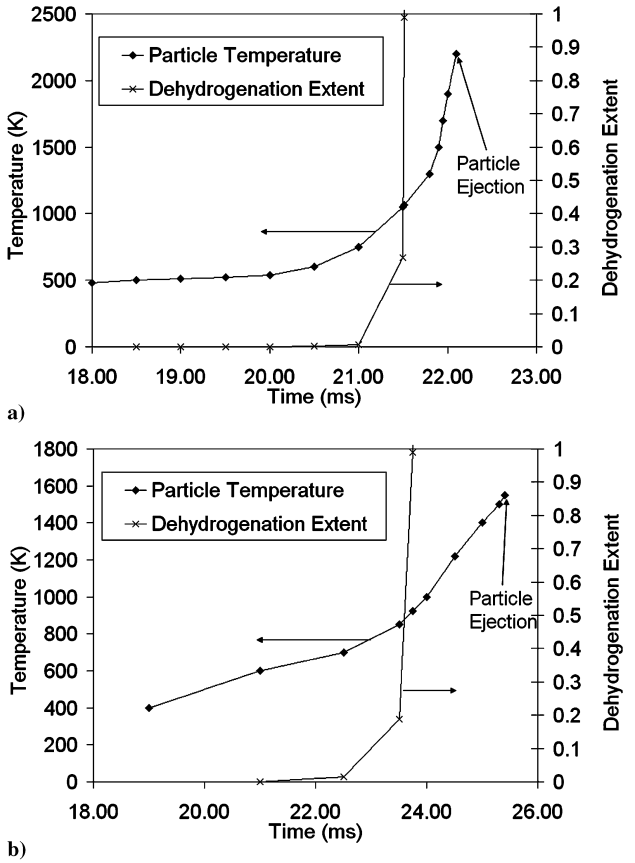

Fig. 13 Plot of particle temperature and dehydrogenation extent vs time for a) an 8 μm particle and b) a 64 μm particle.

the particle is still attached to the propellant surface. An alternative time-temperature history for a 64 μm particle is shown in Fig. 13b. Here, we see that the particle temperature increases more gradually, as the large particle is slowly exposed to the gaseous surface. Whereas this leads to a slightly more gradual dehydrogenation process, the exponential dependence of decomposition on temperature again leads to rapid decomposition once the particle temperature rises to the vicinity of 800 K. This condition is still met while the particle is on the propellant surface. The extrapolation of Eq. (3) shows that the decomposition occurs rapidly relative to the residence time of the particle near the propellant surface once the particle temperature reaches ~700 K. The simulations demonstrate that the particles do indeed reach temperatures considerably higher than this while still in the condensed propellant. Simulations were performed both with no dependence of decomposition time on particle size and with decomposition time proportional to particle size. The actual behavior appears to be somewhere between those two assumptions [7]. Under both situations, dehydrogenation still occurs while the particle is on the propellant surface because of the strong temperature dependence.

Calculations with intermediate particle sizes were performed as well. The results indicate that regardless of particle size, the dehydrogenation of alane occurs when the particle is exposed to the gas phase but still on the propellant surface. This would lead to a situation where the hydrogen would react in the primary flame with the oxidizer and binder in the primary flame zone. Therefore, propellant design should include the hydrogen gas in the stoichiometry of the primary flame zone. The residual aluminum particles will then pass through the primary flame and react in the post flame gases in a similar manner to spherical aluminum particles. It is also possible that the desorption of hydrogen gas from the particle could affect the surface behavior of the propellant, e.g., hydrogen release from the particle could cause the alane particles to eject from the surface sooner because the desorbing gas could disrupt the surface tension holding the particle on the propellant surface. In addition, a significant amount of hydrogen will outgas from the propellant surface, and this process could cause possible changes in the burning surface, including additional surface area or ejection of propellant into the primary flame zone as the hydrogen bubbles from the surface.

The kinetic decomposition model used here is fairly simplistic, and there may be other factors that alter the decomposition rate in a real SRM. First, the extrapolation of the measured rate constant to higher temperatures requires validation. Though there is no evidence in the literature of an alternative high temperature decomposition pathway that may compete with the lower temperature pathway for which we have measured the rate, there is so little work done in this area that a deviation from simple Arrhenius kinetics at higher temperatures may be possible. Further experimental work that can measure fast time scales (e.g., shock tube measurements) would be helpful.

Transport limitations may also affect the dehydrogenation rate. Removal of hydrogen from the alane lattice requires chemical desorption followed by transport out of the solid. At high temperature, desorption may be more rapid than diffusion out of the particle, leading to a longer decomposition time than expected by kinetics alone. In this case, decomposition times would increase with increasing particle size. Again, further experiments at high temperatures would be helpful in determining if this is the case. Of perhaps greater concern is the fact that the alane in a propellant mixture will be at least partially coated with another solid material (binder or oxidizer) which may act to suppress dehydrogenation by allowing a large gas partial pressure to build up in or around the outgassing particle. However, due to the high hydrogen content in alane, this pressure will rapidly build up past the (relatively low) yield stress of the propellant, producing a local gas bubble that will be released very close to the burning propellant surface. Thus, there may be a slight additional delay, but due to the very rapid decomposition rate at the propellant burning surface, very little hydrogen is still expected to remain upon particle release from the burning surface.

V. Conclusions

This study has investigated the decomposition timescales of aluminum hydride and its influence on combustion in a SRM. The following conclusions can be drawn:

1) The decomposition time of alane is exponentially temperature dependent, fitting well to an Arrhenius-style rate equation with a preexponential of 3.29e9 1/s and an activation energy of 97.6 kJ/mol. For example, at 450 K, it takes approximately 65 s for 90% of the hydrogen to desorb from a ~15 μm alane particle. When extrapolated to 1000 K, this relation predicts a decomposition time of 38 μs.

2) Model simulations indicate that alane particles reach sufficiently high temperatures on the propellant surface for full decomposition to occur while the particles are still attached to the surface.

3) The hydrogen desorbed from alane particles will be available to react with the binder and oxidizer in the primary flame zone, and this reaction therefore needs to be considered when modeling combustion chemistry in SRM propellants containing alane.

Acknowledgments

Bazyn, Krier, and Glumac were supported by the Office of Naval Research under contract N00014-01-1-0899. The project monitor is Judah Goldwasser. Wang and Jackson were supported by the U.S. Department of Energy through the University of California under subcontract number B341494.

References

[1] Brower, F. M., Matzek, N. E., Reigler, P. F., Rinn, H. W., Roberts, C. B., Schmidt, D. L., Snover, J. A., and Terada, K., "Preparation and Properties of Aluminum Hydride," *Journal of the American Chemical Society*, Vol. 98, No. 9, 1976, pp. 2450–2453.

[2] Petrie, M. A., Bottaro, J. C., Schmitt, R. J., Penwell, P. E., and Bomberger, D. C., "Preparation of Aluminum Hydride Polymorphs, Particularly Stabilized α-AlH_3," U.S. Patent No. US 6,228,338 B1, 8 May 2001.

[3] Sinke, G. C., Walker, L. C., Oetting, F. L., and Stull, D. R., "Thermodynamic Properties of Aluminum Hydride," *Journal of Chemical Physics*, Vol. 47, No. 8, 1967, pp. 2759–2761.

[4] Cruise, D. R., "Theoretical Computations of Equilibrium Compositions, Thermodynamic Properties, and Performance Characteristics of Propellent Systems," NWC TP 6037, Naval Weapons Center, China Lake, CA, 1991.

[5] Bazyn, T., Eyer, R., Krier, H., and Glumac, N., "Combustion Characteristics of Aluminum Hydride at Elevated Pressure and Temperature," *Journal of Propulsion and Power*, Vol. 20, No. 3, 2004, pp. 427–431.

[6] Ismail, I., and Hawkins, T., "Kinetics of Thermal Decomposition of Aluminuium Hydride: 1—Non-Isothermal Decomposition Under Vacuum and in Inert Atrmosphere (Argon)," *Thermochimica Acta*, Vol. 439, Nos. 1–2, 2005, pp. 32–43.

[7] Tarasov, V., Muravlev, Y., Bakum, S., and Novikov, A., "Kinetics of Formation of Metallic Aluminum upon Thermal and Photolytic Decomposition of Aluminum Trihydride and Trideuteride as Probed by NMR," *Doklady Physical Chemistry (Translation of the physical chemistry section of Doklady Akademii Nuak)*, Vol. 393, Nos. 4–6, 2003, pp. 353–356.

[8] Mikhailov, Y., Galitsin, Y. G., Boldyrev, V., and Pimenov, Y., "Optical Absorption Spectra and Their Behavior in Photolysis and Thermolysis of Aluminum Hydride," *Optics and Spectroscopy (USSR)*, Vol. 39, No. 6, 1975, pp. 651–653.

[9] Mikhailov, Y., Galitsyn, G., Khairetdinov, E., Poshevnev, V., and Boldyrev, V., "Dark Electrical Donductivity of Aluminum Hydride," *Neorganicheskie Materialy*, Vol. 15, No. 1, 1979, pp. 72–75.

[10] Mikhailov, Y., Galitsyn, G., and Boldyrev, V., "Effect of Preliminary UV Irradiation on the Thermal Decomposition of Aluminum Hydride," *Kinetics and Catalysis*, Vol. 17, No. 3, 1976, pp. 608–611.

[11] Poshevnev, V., Galitsyn, Y., Mikhailov, R., and Boldyrev, V., "Kinetics of Hydrogen Gas Evolution in the Thermolysis of Aluminum Hydride," *Doklady Physical Chemistry (Translation of the physical chemistry section of Doklady Akademii Nuak)*, Vol. 256, No. 4, 1981, pp. 904–908.

[12] Herley, P., and Irwin, R., "A Preliminary Study of the Thermal and Photolytic Decomposition of Aluminum Hydride Powder," *Journal of the Physics and Chemistry of Solids*, Vol. 39, No. 9, 1978, pp. 1013–1015.

[13] Herley, P., Christofferson, O., and Irwin, R., "Decomposition of α-Aluminum Hydride Powder," *Journal of Physical Chemistry*, Vol. 85, No. 13, 1981, pp. 1874–1881.

[14] Zakharov, V., and Tskhai, A., "The Thermal Transformations of Ether Addition Compounds of Aluminum Hydride," *Russian Journal of Inorganic Chemistry*, Vol. 37, No. 9, 1992, pp. 1935–1940.

[15] Knott, G. M., Jackson, T. L., and Buckmaster, J., "The Random Packing of Heterogeneous Propellants," *AIAA Journal*, Vol. 39, No. 4, 2001, pp. 678–686.

[16] Kochevets, S., Buckmaster, J., Jackson, T. L., and Hegab, A., "Random Packs and Their Use in the Modeling of Heterogeneous Solid Propellant Combustion," *Journal of Propulsion and Power*, Vol. 17, No. 4, 2001, pp. 883–891.

[17] Chen, M., Buckmaster, J., Jackson, T. L., and Massa, L., "Homogenization Issues and the Combustion of Heterogeneous Solid Propellants," *Proceedings of the Combustion Institute*, Vol. 29, 2002, pp. 2923–2929.

[18] Jackson, T. L., and Buckmaster, J., "Heterogeneous Propellant Combustion," *AIAA Journal*, Vol. 40, No. 6, 2002, pp. 1122–1130.

[19] Massa, L., Jackson, T. L., and Short, M., "Numerical Solution of Three-Dimensional Heterogeneous Solid Propellants," *Combustion Theory and Modelling*, Vol. 7, No. 3, 2003, pp. 579–602.

[20] Massa, L., Jackson, T. L., and Buckmaster, J., "New Kinetics for a Model of Heterogeneous Propellant Combustion," *Journal of Propulsion and Power*, Vol. 21, No. 5, 2005, pp. 914–924.

[21] Wang, X., Jackson, T. L., and Massa, L., "Numerical Simulation of Heterogeneous Propellant Combustion by a Level Set Method," *Combustion Theory and Modelling*, Vol. 8, No. 2, 2004, pp. 227–254.

[22] Wang, X., and Jackson, T. L., "The Numerical Simulation of Two-Dimensional Aluminized Composite Solid Propellant Combustion," *Combustion Theory and Modelling*, Vol. 9, No. 1, 2005, pp. 171–197.

S. Son
Associate Editor